

## Mechanistic Evidence for an $\alpha$ -Oxoketene Pathway in the Formation of $\beta$ -Ketoamides/Esters via Meldrum's Acid Adducts

Feng Xu,<sup>\*,†</sup> Joseph D. Armstrong III,<sup>\*,†</sup> George X. Zhou,<sup>\*,‡</sup> Bryon Simmons,<sup>†</sup>  
David Hughes,<sup>†</sup> Zhihong Ge,<sup>‡</sup> and Edward J. J. Grabowski<sup>†</sup>

Contribution from the Departments of Process Research and Analytical Research,  
Merck Research Laboratory, Rahway, New Jersey 07065

Received June 14, 2004; E-mail: feng\_xu@merck.com

**Abstract:** A practical, one-pot process for the preparation of  $\beta$ -keto amides via a three-component reaction, including Meldrum's acid, an amine, and a carboxylic acid, has been developed. Key to development of an efficient, high-yielding process was an in-depth understanding of the mechanism of the multistep process. Kinetic studies were carried out via online IR monitoring and subsequent principal component analysis which provided a means of profiling the concentration of both the anionic and free acid forms of the Meldrum's acid adduct **6** in real time. These studies, both in the presence and absence of nucleophiles, strongly suggest that formation of  $\beta$ -keto amides from acyl Meldrum's acids occurs via  $\alpha$ -oxoketene species **2** and rule out other possible reaction pathways proposed in the literature, such as via protonated  $\alpha$ -oxoketene intermediates **3** or nucleophilic addition–elimination pathways.

### Introduction

$\beta$ -Keto esters and amides are versatile intermediates in organic synthesis and often are prepared from acyl Meldrum's acid adducts.<sup>1</sup> This method involves reaction of Meldrum's acid with activated carboxylic acids followed by decarboxylation in the presence of nucleophiles such as alcohols or amines (Scheme 1). The ability of readily available acyl Meldrum's acid adducts to react with various nucleophiles allows quick access to a variety of functionalized compounds. Application of this methodology in synthetic chemistry has been widely exploited; however, the mechanism is not well understood.<sup>1–4</sup> Four tentative reaction pathways have been proposed: (1) nucleophilic addition–elimination pathway via intermediate **1**;<sup>5</sup> (2) formation of  $\alpha$ -oxoketene **2**;<sup>3,5b,6</sup> (3) formation of protonated  $\alpha$ -oxoketene **3**;<sup>2</sup> and (4) reaction via intermediate **4** (Figure 1).<sup>6a,7</sup>

$\alpha$ -Oxoketenes **2** have been the focus of numerous theoretical and experimental studies.<sup>8</sup> They have been observed by thermolysis of Meldrum's acid derivatives in boiling diphenyl ether

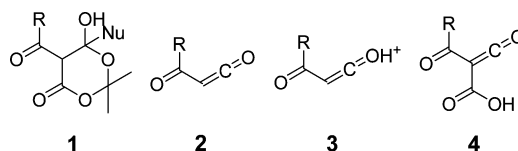
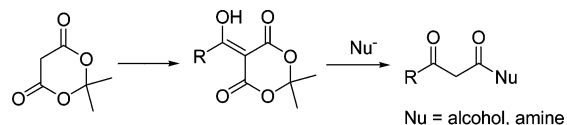


Figure 1. Possible reaction intermediates proposed in the literature.

### Scheme 1. Preparation of $\beta$ -Keto Esters and Amides from Acyl Meldrum's Acids



(259 °C)<sup>9</sup> or under flash vacuum pyrolysis condition (600 °C, 0.01 Torr).<sup>10,11</sup> In light of these studies,<sup>1</sup> **2** has been suggested as a possible intermediate in reactions in which acyl Meldrum's acid adducts react with amines, alcohols, and imines, etc., although the alternative pathway through nucleophilic addition to intermediate **1** followed by elimination cannot be excluded.<sup>5b,6</sup>

<sup>†</sup> Department of Process Research.

<sup>‡</sup> Department of Analytical Research.

- (1) For reviews, see: (a) Far, A. D. *Angew. Chem., Int. Ed. Engl.* **2003**, *42*, 2340–2348. (b) Gaber, A. E. M.; McNab, H. *Synthesis* **2001**, 2059–2074. (c) Chen, B. C. *Heterocycles* **1991**, *32*, 529–597. (d) Huang, X. *Youji Huaxue* **1986**, 329–334.
- (2) Emtenas, H.; Alderin, L.; Almqvist, F. *J. Org. Chem.* **2001**, *66*, 6756–6761.
- (3) Emtenas, H.; Soto, G.; Hultgren, S. J.; Marshall, G. R.; Almqvist, F. *Org. Lett.* **2000**, *2*, 2065–2067.
- (4) The mechanism involving acyl Meldrum's acids in solution was never clarified. It is often to have several proposed reaction pathways in the same publication.
- (5) For examples, see: (a) Pak, C. S.; Yang, H. C.; Choi, E. B. *Synthesis* **1992**, 1213–1214. (b) Svetlik, J.; Goljer, I.; Turecek, F. *J. Chem. Soc., Perkin Trans. 1* **1990**, 1315–1318. (c) Sato, M.; Yoneda, N.; Katagiri, N.; Watanabe, H.; Kaneko, C. *Synthesis* **1986**, 672–674. (d) Oikawa, Y.; Sugano, K.; Yonemitsu, O. *J. Org. Chem.* **1978**, *43*, 2087–2088.

- (6) For additional examples, see: (a) Yamamoto, Y.; Watanabe, Y.; Ohnishi, S. *Chem. Pharm. Bull.* **1987**, *35*, 1860–1870. (b) Sato, M.; Ogasawara, H.; Yoshizumi, E.; Kato, T. *Chem. Pharm. Bull.* **1983**, *31*, 1902–1909. (c) Sato, M.; Ogasawara, H.; Yoshizumi, E.; Kato, T. *Heterocycles* **1982**, *17*, 297–300.
- (7) (a) Hamilakis, S.; Kontonassios, D.; Sandris, C. *J. Heterocycl. Chem.* **1996**, *33*, 825–829. (b) Sato, M.; Takayama, K.; Abe, Y.; Furuya, T.; Inukai, N.; Kaneko, C. *Chem. Pharm. Bull.* **1990**, *38*, 336–339. (c) Yamamoto, Y.; Watanabe, Y. *Chem. Pharm. Bull.* **1987**, *35*, 1871–1879.
- (8) For recent reviews, see: (a) Tidwell, T. T. *Ketenes*; John Wiley & Sons: New York, 1995. (b) Wentrup, C.; Heilmayer, W.; Kollenz, G. *Synthesis* **1994**, 1219–1249. (c) Tidwell, T. T. *Acc. Chem. Res.* **1990**, *23*, 273–279.
- (9) Cassis, R.; Tapia, R.; Valderrama, J. A. *Synth. Commun.* **1985**, *15*, 125–133.
- (10) Gordon, H. J.; Martin, J. C.; McNab, H. *J. Chem. Soc., Chem. Commun.* **1983**, 957–958.
- (11) Bibas, H.; Kappe, C. O.; Wong, M. W.; Wentrup, C. *J. Chem. Soc., Perkin Trans. 2* **1998**, 493–498.

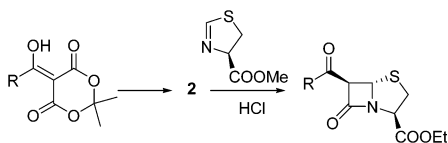
Almqvist et al.<sup>3</sup> suggested that formation of  $\beta$ -lactams<sup>12</sup> is a [2 + 2] product of  $\alpha$ -oxoketene **2** and a thiazoline. Subsequently, they also proposed that 2-pyridinone<sup>13</sup> is formed through protonated ketene intermediate **3** when branched imines are subjected to the same reaction conditions as for the preparation of  $\beta$ -lactams.<sup>2</sup> However, other literature examples suggest pathways not involving **2** are also viable. For example, pyranones can be prepared via [2 + 4] addition of vinyl ethers with  $\alpha$ -oxoketenes **2** generated by thermolysis of dioxinones.<sup>14</sup> In contrast, treatment of acyl Meldrum's adducts with vinyl ethers (benzene, 80 °C) results in formation of pyrandiones rather than pyranones.<sup>14</sup> Similarly, ketone-exchanged products, 1,3-oxazinediones,<sup>6a</sup> are formed when acyl Meldrum's acids are treated with cyclohexanone in refluxing benzene. Apparently, reaction pathways other than via  $\alpha$ -oxoketene **2** are involved to form pyrandiones<sup>14</sup> as well as 1,3-oxazinediones<sup>6a</sup> since decarboxylation does not occur during the reaction. Yamamoto et al.<sup>6a</sup> proposed that the intermediate **4** or its zwitterionic tautomers could be responsible for the formation of 1,3-oxazinones while also suggesting that acyl Meldrum's adducts are a good source of  $\alpha$ -oxoketene **2**. Given that these reactions are poorly understood and to improve the versatility and efficiency of these reactions, we undertook a detailed mechanistic study to better define the reaction pathway and to gain insight on the factors which influence the reaction.

## Results and Discussion

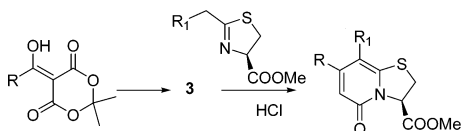
In conjunction with a recent drug development program, we required an efficient preparation of  $\beta$ -keto amide **8**, which we envisioned could be accomplished via coupling of the three readily available components as shown in Scheme 2. In the first part of this section, we describe the design and development of a process to prepare **8** in an efficient, one-pot process. The observations made during the development of this process provided the basis for an in-depth examination of the mechanistic aspects of the reaction, which are detailed in the latter part of this section. The combination of online IR monitoring and principal component analysis made it possible to profile the concentration of both the anionic and free acid forms of the Meldrum's adduct **6** in real time for kinetic studies, which provided a critical tool for delineating the mechanism of this complex reaction sequence.

**One-Pot, Three-Component Coupling and Key Observations.** The synthetic process to couple the carboxylic acid **5**, Meldrum's acid, and the triazole **7** consists of three key steps:

(12) Cf. ref 3.

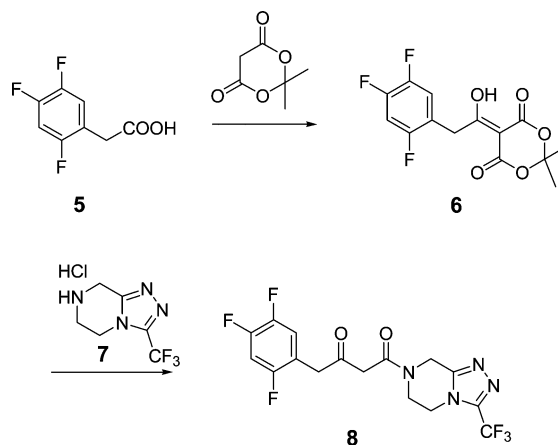


(13) Cf. ref 2.



(14) Zawacki, F. J.; Crimmins, M. T. *Tetrahedron Lett.* **1996**, *37*, 6499–6502.

## Scheme 2. Preparation of $\beta$ -Keto Amide **8**



carboxylic acid activation, reaction of the activated acid with Meldrum's acid, followed by reaction with the amine and decarboxylation. After preliminary optimization, **6** was prepared by adding 1.1–1.2 equiv of pivaloyl chloride to a solution of Meldrum's acid, the carboxylic acid **5**, catalytic DMAP, and *i*-Pr<sub>2</sub>NEt in dimethylacetamide (Me<sub>2</sub>NAC) or MeCN as solvent, at ambient temperature followed by warming to 55 °C. Preliminary studies indicated **6** was unstable in acidic media at ambient temperature<sup>15</sup> but was quite stable in basic solution. To overcome the instability of the free acid of **6** which would occur upon attempted isolation, a one-pot process to prepare **8** was required. However, when **6** was formed in the presence of 3 equiv of *i*-Pr<sub>2</sub>NEt in 95% yield, and treated directly with 1.0 equiv of triazole HCl salt **7**, the decarboxylation/aminolysis reaction was slow and stalled at about 80% conversion. This was remedied by reducing the amount of *i*-Pr<sub>2</sub>NEt to 2.1 equiv, which is sufficient to neutralize the HCl and adduct **6** ( $pK_a = 3.1$ )<sup>16</sup> generated during the reaction, but not *t*-BuCO<sub>2</sub>H ( $pK_a = 5.0$ ), which has the highest  $pK_a$  of the three acids formed during the reaction. Under these conditions, we found that formation of **6** still performed well (95% yield, 97% conversion) and the decarboxylation/aminolysis now proceeded smoothly at 70 °C to achieve 98% conversion within 6 h after 1 equiv of triazole HCl salt **7** was added. However, the overall reaction process is quite sensitive to the initial *i*-Pr<sub>2</sub>NEt charge since the base has opposing effects on the two steps. The rate of decarboxylation decreases as the initial base charge increases. If the base charge is <1.9 equiv, formation of **6** suffers from conversion and yield, while the decarboxylation is very fast and reaches completion within 2 h at 70 °C and the overall yield for the two steps is <85%. If the base charge is >2.2 equiv, >98% conversion for formation of **6** can be achieved, while the decarboxylation is slow and cannot reach full conversion at 70 °C. Thus, the amount of base must be carefully balanced (2.0–2.1 equiv) to achieve maximum conversion and yield.

**Acid Effects in the One-Pot Process.** The observations outlined above suggested the decarboxylation/amination reaction required a somewhat acidic medium for optimum results. Likewise, a careful review of literature reports for the preparation of  $\beta$ -keto amides revealed that the amine component was

(15) It is known that acyl Meldrum's acids are not always stable. For example, see ref 5b.

(16) Measured by titration in water at ambient temperature.

always undercharged relative to the acyl Meldrum's acid intermediate, again suggesting that slightly acidic conditions might be beneficial.<sup>5</sup> Several acids of varying  $pK_a$  were screened to understand the role of acidity on decarboxylation. Acids with  $pK_a$  of  $<3.5$ , including HCl,  $\text{MeSO}_3\text{H}$ ,  $\text{CF}_3\text{CO}_2\text{H}$ , and 2- $\text{O}_2\text{N}$ - and 3- $\text{O}_2\text{N}$ - $\text{C}_6\text{H}_4\text{CO}_2\text{H}$ , afforded conversions of  $>95\%$  within 6 h at 55 °C. The weaker acids HOAc and  $t\text{-BuCO}_2\text{H}$  gave conversions of only 61% and 20%, respectively. Thus, acids that can protonate adduct **6**, which has an aqueous  $pK_a$  of 3.1, are effective in promoting rapid reaction, suggesting the free acid form of **6** is the reactive intermediate.

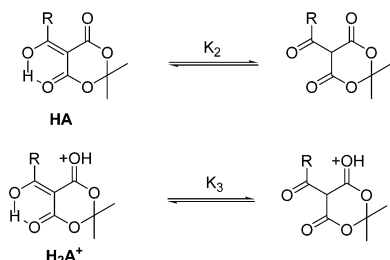
The reaction was further optimized with  $\text{CF}_3\text{CO}_2\text{H}$  (TFA) chosen as an acid having appropriate acidity. The optimized protocol involves formation of **6** with pivaloyl chloride and Meldrum's acid and the addition of **7**, followed by addition of TFA, typically 0.3 equiv. In this way, the significant aminolysis rate variation caused by the slight changes in  $i\text{-Pr}_2\text{NEt}$  charge is minimized after the TFA "pH adjustment". Finally, the decarboxylation/aminolysis reaction is carried out at lower temperature (50 °C vs the previous 70 °C).<sup>17</sup>

These noteworthy observations made during process development prompted us to study the reaction in more detail. In the mechanistic studies described below, we provide conclusive evidence that the reaction of Meldrum's acid adducts such as **6** proceed via an  $\alpha$ -oxoketene pathway. The mechanistic work is divided into two major sections: kinetic studies and model studies.

**Kinetic Studies on Self-Decomposition of Acyl Meldrum's Adduct 6.** Our kinetic studies began with an investigation of the decomposition of **6** in the absence of an added nucleophile, which can proceed either via the neutral compound (path A, Scheme 3) or the protonated species (path B, Scheme 3). As discussed below, these pathways can be distinguished based on the response of the kinetics to added acid or base.<sup>18</sup>

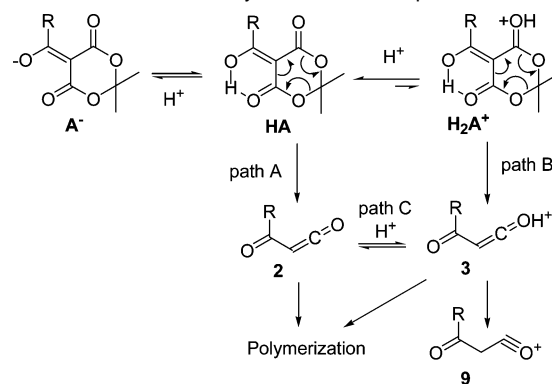
(17) One-pot process procedure: 2,4,5-Trifluorophenylacetic acid (**5**, 2.5 kg, 13.15 mol), Meldrum's acid (2.09 kg, 14.46 mol), and DMAP (128.5 g, 1.052 mol) were charged into a 50 L three-neck flask. Acetonitrile (7.5 L) was added in one portion at room temperature.  $N,N$ -Diisopropylethylamine (4.92 L, 28.27 mol) was added in portions at room temperature while maintaining the temperature below 50 °C. Pivaloyl chloride (1.78 L, 14.46 mol) was added dropwise over 1–2 h while maintaining the temperature below 55 °C. The reaction was aged at 45–50 °C for 2–3 h. Triazole hydrochloride **7** (3.01 kg, 13.2 mol) was added in one portion at 40–50 °C. Trifluoroacetic acid (303 mL, 3.95 mol) was added dropwise, and the reaction solution was aged at 50–55 °C for 6 h. 90% solution assay yield of **8**. This process has been successfully and reproducibly demonstrated in 300 kg scales.

(18) To have a less complicated consideration, all the tautomers, rotamers, as well as resonance structures are not specifically considered here. For example, although the following equilibria can be included in the kinetic analyses, the outcome reaction rate can be expressed as:  $kK_1K_3[\text{HA}]^2/[\text{A}^-]$  for pathway B and  $kK_2[\text{HA}]$  for pathway A, which result in the same kinetic effects on  $[\text{HA}]$  or  $[\text{A}^-]$  as described in the text.

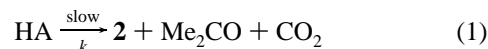


To have more focused discussion in the text, detailed kinetic analyses of all other possible mechanisms, which can be done as described in the text, are not listed here.

**Scheme 3.** Possible Pathways for Self-Decomposition<sup>18</sup>

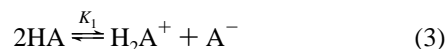


For pathway A, the reaction rate constants will be unaffected by added acid or base, as shown in eqs 1 and 2.



$$\text{rate} = k[\text{HA}] \quad (2)$$

For pathway B, the following equations apply:



$$[\text{H}_2\text{A}^+] = \frac{K_1[\text{HA}]^2}{[\text{A}^-]}$$

$$\text{rate} = k[\text{H}_2\text{A}^+] = \frac{kK_1[\text{HA}]^2}{[\text{A}^-]} \quad (5)$$

In the absence of acid or base,  $[\text{H}_2\text{A}^+] = [\text{A}^-]$ . Thus,  $[\text{H}_2\text{A}^+] = (K_1)^{1/2}[\text{HA}]$ . Therefore

$$\text{rate} = k[\text{H}_2\text{A}^+] = k(K_1)^{1/2}[\text{HA}] \quad (6)$$

If  $<1$  equiv of base **B** is added to the system,  $\text{A}^-$  would increase and lead to a reduced rate (eq 5).



In the presence of a strong acid the equilibrium (eq 3) is shifted and  $[\text{H}_2\text{A}^+]$  is increased. Therefore, the reaction rate would increase.

In addition, protonation of ketenes has been studied both theoretically and experimentally.<sup>8,19</sup> The preferred protonation of ketene is at  $\text{C}_\beta$  to afford the acylium ion **9** instead of **3**. In the gas phase, **9** is lower in energy than the  $\alpha$ -protonated ketene **3**.<sup>8,19–21</sup> It is unlikely that **3** can be formed through direct protonation of **2** via pathway C since this process has a high energy barrier and **3** is disfavored thermodynamically.<sup>21</sup>

(19) For leading references, see: (a) Gong, L.; McAllister, M. A.; Tidwell, T. *J. Am. Chem. Soc.* **1991**, *113*, 6021–6028. (b) Lien, M. H.; Hopkinson, A. C. *J. Org. Chem.* **1988**, *53*, 2150–2154. (c) Armitage, M. A.; Higgins, M. J.; Lewars, E. G.; March, R. E. *J. Am. Chem. Soc.* **1980**, *102*, 5064–5068.

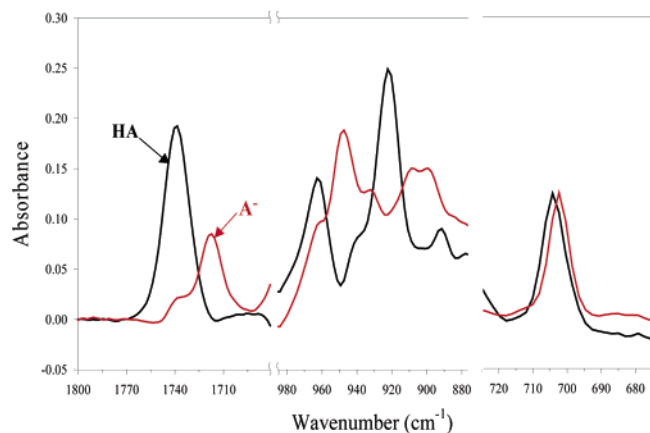


**Figure 2.** Extracted spectra of the free acid (**HA**) and anion (**A<sup>-</sup>**, *i*-Pr<sub>2</sub>NEt salt) of **6** obtained in Me<sub>2</sub>NAC.

At this point, it became clear that *the capability to obtain the kinetic profile of the free acid 6 as well as its anionic form was essential to understand the reaction pathway*. Therefore, attempts to quantify the free acid and its anionic form in solution by applying online IR techniques were initiated. Titration with *i*-Pr<sub>2</sub>NEt showed that the free acid **6** was stoichiometrically converted to its anionic form as expected on the basis of the several unit differences of  $pK_a$ 's between **6** and *i*-Pr<sub>2</sub>NEt. Although the IR spectra of the free acid **6** and its anion are substantially different, the overlapping peaks in the online IR spectra obtained during a reaction or titration are very subtle and make obtaining the kinetic profiles of the free acid **6** and its anion quite difficult. To fully distinguish each component in the complex mixture, a more sophisticated data analysis method had to be applied in order to resolve each component over the entire reaction period.

The method we chose was principal component analysis, an algorithm that has been used to extract chemical and process information from reaction spectra.<sup>22,23</sup> To extract the spectra of both free acid **6** and its anionic form, principal component analyses were first performed on the titration spectra of free acid **6** with *i*-Pr<sub>2</sub>NEt, using ConCIRt (version 2, from ASI Applied Systems, Millersville, MD). After several attempts, optimal spectral regions (1800–1680, 985–875, and 725–675 cm<sup>-1</sup>) containing major spectral features of both acid **6** and its anion, and having the least interferences by other coexisting species, were identified. The component spectra of the free acid **6** and its anion within these three optimal regions were obtained and are illustrated in Figure 2. Peaks at 704.3, 922.3, and 1739.4 cm<sup>-1</sup> represent the free acid **6** while peaks at 702.3, 947.7, and 1717.6 cm<sup>-1</sup> correspond to the anionic form of **6**.<sup>24</sup> Thus, quantitative monitoring of the real time concentration change

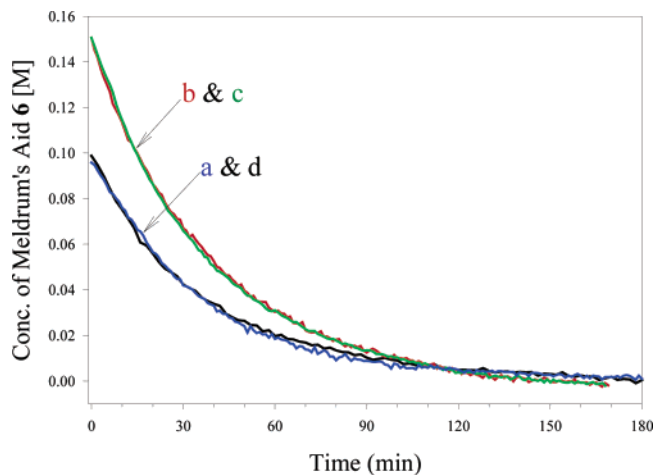
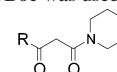


**Figure 3.** Self-decomposition of the free acid **6** in Me<sub>2</sub>NAC. Plots of concentration of **HA** vs time: (a) **6** itself at 51.5 °C; (b) in the presence of 0.5 equiv of TFA at 48.3 °C; (c) in the presence of 1.0 equiv of TFA at 48.8 °C; (d) in the presence of 0.5 equiv of *i*-Pr<sub>2</sub>NEt at 52.5 °C.

**Table 1.** Measured  $k_{\text{obs}}$ 's in Me<sub>2</sub>NAC with Isolated **6**

entry	substrates	additive	$k_{\text{obs}} \times 10^{-4}$ (s <sup>-1</sup> )	T (°C)	yield <sup>c</sup> (%)
1	BocNHOBoc <sup>a</sup>		3.93	50.8	<b>10</b> , 78
2	BocNHOBoc <sup>b</sup>		3.35	50.1	<b>10</b> , 78
3	<i>n</i> -PrOH		4.18	51.0	<b>11</b> , 97
4	PhNH <sub>2</sub>		4.04	50.8	<b>12</b> , 92
5	piperidine		4.78	50.9	<b>13</b> , <sup>e</sup> 78
6	<b>7</b> <sup>d</sup>		1.14	41.1	<b>8</b> , 91
7	<b>7</b> <sup>d</sup>		4.81	51.4	<b>8</b> , 91
8	<b>7</b> <sup>d</sup>		17.0	61.8	<b>8</b> , 90
9	none	none	4.09	51.5	
10	none	TFA (0.5 equiv)	4.37	48.3	
11	none	TFA (1.0 equiv)	4.37	48.8	
12	none	<i>i</i> -Pr <sub>2</sub> NEt (0.5 equiv)	4.68	52.5	

<sup>a</sup> 2 equiv of BocNHOBoc was used. <sup>b</sup> 1 equiv of BocNHOBoc was used. <sup>c</sup> Isolated yield. <sup>d</sup> Free base. <sup>e</sup> **13** (R = 2,4,5-trifluorobenzyl) =



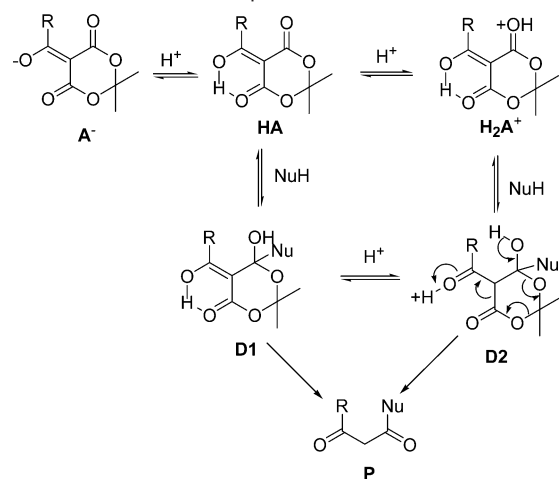
of **HA** and **A<sup>-</sup>** in the reaction system became possible by feeding/using the above extracted spectra (Figure 2).

With an analytical method in hand, kinetic studies were initiated. Due to the solubility limitation of **6** in acetonitrile, the self-decomposition kinetic studies were studied first by using isolated adduct **6** in a homogeneous Me<sub>2</sub>NAC solution, which provided a simplified system by eliminating all the acid–base equilibria that exist in the one-pot process solution. As mentioned above, preparation of **8** is equally effective in either MeCN or Me<sub>2</sub>NAC. As shown in Figures 3 and S1 (Supporting Information), a first-order dependence in the acid form **6** (**HA**) was clearly observed, with a  $k_{\text{obs}}$  of  $4.09 \times 10^{-4} \text{ s}^{-1}$ .

In addition, the kinetic profiles for the self-decomposition of **6** in the absence/presence of TFA or *i*-Pr<sub>2</sub>NEt (Figure 3; Table 1, entries 9–12) indicate that acid or base have almost no effect on the rate constants. The observed first-order kinetics in **HA** only, along with the lack of catalysis by TFA, allowed us to rule out the pathway via protonated ketene **3** for the decomposition of acyl Meldrum's adducts.<sup>25</sup>

**Kinetic Evidence against Nucleophilic Addition–Elimination Mechanism.** Based on the kinetics described above, the self-decomposition of **6** is consistent with reaction via an  $\alpha$ -oxoketene intermediate. However, for reactions in the pres-

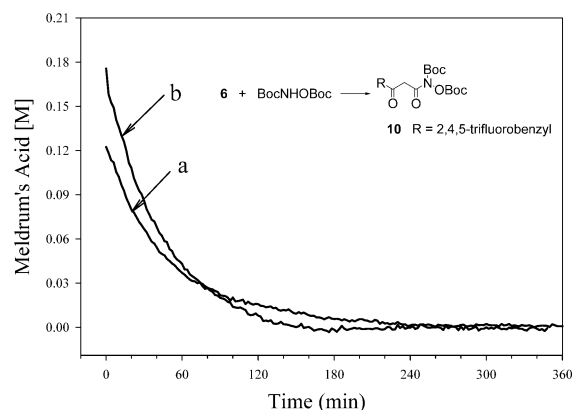
- (20) (a) Birney, D. M. *J. Org. Chem.* **1994**, *59*, 2557–2564. (b) Tortajada, J.; Berthomieu, D.; Morizur, J.-P.; Audier, H.-E. *J. Am. Chem. Soc.* **1992**, *114*, 10874–10880. (c) Leung-Toung, R.; Peterson, M. R.; Tidwell, T. T.; Csizmadia, I. G. *J. Mol. Struct.* **1989**, *183*, 319–330. (d) Bouchoux, G.; Hppilliard, Y. *J. Phys. Chem.* **1988**, *92*, 5869–5874.
- (21) ) As reported, 43 kcal/mol gap exists between CH<sub>3</sub>C=O<sup>+</sup> and CH<sub>2</sub>=C=O<sup>+</sup>H. See: (a) Nobes, R. H.; Bouma, W. J.; Radom, L. *J. Am. Chem. Soc.* **1983**, *105*, 309–314. (b) Vogt, J.; Williamson, A. D.; Beauchamp, J. L. *J. Am. Chem. Soc.* **1978**, *100*, 3478–3483.
- (22) Malinowski, E. H.; Howery, D. G. *Factor Analysis in Chemistry*; John Wiley & Sons: New York, 1980.
- (23) Cameron, M.; Zhou, G. X.; Hicks, M. B.; Antonucci, V.; Ge, Z.; Lieberman, D. R.; Lynch, J. E.; Shi, Y.-J. *J. Pharm. Biomed. Anal.* **2002**, *28*, 137–144.
- (24) The obtained online IR kinetic profiles of the combination of anion and free acid form of **6** as well as the formation of the product matched very well with the HPLC kinetic profile as shown later on in Figure 7.

**Scheme 4.** Possible Nucleophilic Addition–Elimination Pathway<sup>18</sup>

ence of a nucleophile, the nucleophilic addition–elimination through intermediates such as **D1** or **D2**, formed from **HA** or **H<sub>2</sub>A<sup>+</sup>**, could become the preferred pathway (Scheme 4). Given that proton exchange steps are fast, the addition–elimination step or possibly the following fragmentation of **D1** or **D2** would likely be the rate-determining step. Reaction rates or  $k_{\text{obs}}$ 's should be different if nucleophilic addition was involved in the reaction or if fragmentation of an intermediate already incorporating the nucleophile was the rate-limiting step.

As outlined above, isolated acyl Meldrum's adducts react with amines to afford the corresponding  $\beta$ -ketoamides. More interestingly, nonbasic amine derivatives, such as carbamates,<sup>26</sup> amides,<sup>27</sup> and hydroxylamines,<sup>28</sup> as well as alcohols, can also react with these adducts to effectively provide the corresponding 1,3-dicarbonyl compounds. To investigate the effect of the nature of the nucleophile, we selected a variety of basic and nonbasic nucleophiles as reaction partners. We initiated these studies with BocNHOBoc since it is nonbasic and is a much weaker bulky nucleophile than the triazole **7**. Comparison of the  $k_{\text{obs}}$ 's with other weak or strong nucleophiles would reveal whether nucleophilic addition or the following elimination is involved in the rate-determining step.

Thus, **6** was treated with 1 or 2 equiv of BocNHOBoc in Me<sub>2</sub>Nac at 50 °C for 4 h to give **10** in 70% yield.<sup>29</sup> Kinetic studies were carried out by online IR. As shown in Figures 4 and S2 (Supporting Information), first-order kinetics in the free acid **6** and zero-order in BocNHOBoc were clearly observed. The yield and rate were almost identical when 1 or 2 equiv of BocNHOBoc was used. The  $k_{\text{obs}}$ 's (Table 1, entries 1–2) are very close to those measured for the self-decomposition of **6**, in which the rate-determining step is likely the formation of  $\alpha$ -oxoketene **2**.<sup>30</sup> To conclude, the  $k_{\text{obs}}$ 's and the observed first-

**Figure 4.** Plots of concentration of acid form **HA** in Me<sub>2</sub>Nac vs time: (a) in the presence of 1.0 equiv of BocNHOBoc at 50.1 °C; (b) in the presence of 2.0 equiv of BocNHOBoc at 50.8 °C.

order kinetics in **HA** do not support the nucleophilic addition–elimination mechanism and are consistent with a pathway via the oxo-ketene **2** (Figure 4).

These studies were extended with aniline, piperidine, triazole free base **7**, and *n*-propanol as nucleophiles. Note that aniline and triazole **7** ( $pK_{\text{a}} = 4.0$  in water<sup>16</sup>) have similar  $pK_{\text{a}}$ 's.

Introduction of an undercharge of a basic nucleophile such as an amine introduces a new fast acid–base equilibrium (eq 8)



In this case, [HA] is constant before most of **Nu** is consumed (vide infra).<sup>31</sup> Therefore, eqs 2 and 5 would result in different kinetic profiles. As outlined above, the anionic form **A<sup>-</sup>** is very stable and will not react with amines. Negative first-order kinetics in **A<sup>-</sup>** would be observed if a protonated  $\alpha$ -oxoketene is involved in the main reaction pathway. Otherwise, given that the acid–base equilibrium is rapid, pseudo-zero-order in [A<sup>-</sup>] would be expected. Online IR to probe the reaction kinetic profiles again became our tool of choice to differentiate the concentration changes of the anionic form **A<sup>-</sup>** and the free acid form **HA** during the reaction.

Use of *n*-propanol (Figure 5a) resulted in first-order kinetics in **HA**, which was identical to the kinetics observed with the carbamate BocNHOBoc. Use of the triazole **7**, aniline, or piperidine resulted in pseudo-zero-order kinetics in **A<sup>-</sup>**. As shown in Figure 5b, the observed concentration profile of the free acid form **HA** is almost unchanged until the majority of the anionic form **A<sup>-</sup>** is consumed, due to the rapid acid–base proton exchange (eq 8). Triazole **7**, aniline, piperidine, *n*-PrOH, and BocNHOBoc all gave very similar  $k_{\text{obs}}$ 's, which closely matched those measured for the self-decomposition of **6**. The  $k_{\text{obs}}$ 's (Table 1) further confirmed that nucleophiles such as amines, alcohols, carbamates, etc. do not react directly with **HA** or **H<sub>2</sub>A<sup>+</sup>**. The fact that the reaction rate is zero order in **A<sup>-</sup>** in the presence of amine nucleophiles (piperidine, aniline, **7**) also implies that the main reaction pathway is through an  $\alpha$ -oxo-ketene rather than a protonated  $\alpha$ -oxoketene intermediate.

Kinetic studies were also carried out at different reaction temperatures (Table 1, entries 6–8) to determine the activation

(25) A stepwise formation of the oxo-ketene by loss of acetone to form intermediates such as **4**, followed by decarboxylation, cannot be ruled out. The fact that the reaction rate is unaffected by the increasing concentration of acetone formed during the reaction provides some evidence against the pathway via intermediates such as **4**, if reversible formation<sup>6a</sup> of these intermediates is the rate-determining step.

(26) Sorensen, U. S.; Falch, E.; Krosgaard-Larsen, P. *J. Org. Chem.* **2000**, *65*, 1003–1007.

(27) Yamamoto, Y.; Ohnishi, S.; Azuma, Y. *Chem. Pharm. Bull.* **1982**, *30*, 3505–3512.

(28) Mohri, K.; Oikawa, Y.; Hirao, K.-I.; Yonemitsu, O. *Chem. Pharm. Bull.* **1982**, *30*, 3097–3105; *Heterocycles* **1982**, *19*, 515–520, 521–524.

(29) Similar yields were reported in the literature for other substrates.

(30) Shelkov, R.; Nahmany, M.; Melman, A. *J. Org. Chem.* **2002**, *67*, 8975–8982.

(31) For more detailed discussions, see “Kinetic profile in the ‘real’ one-pot solution” section.

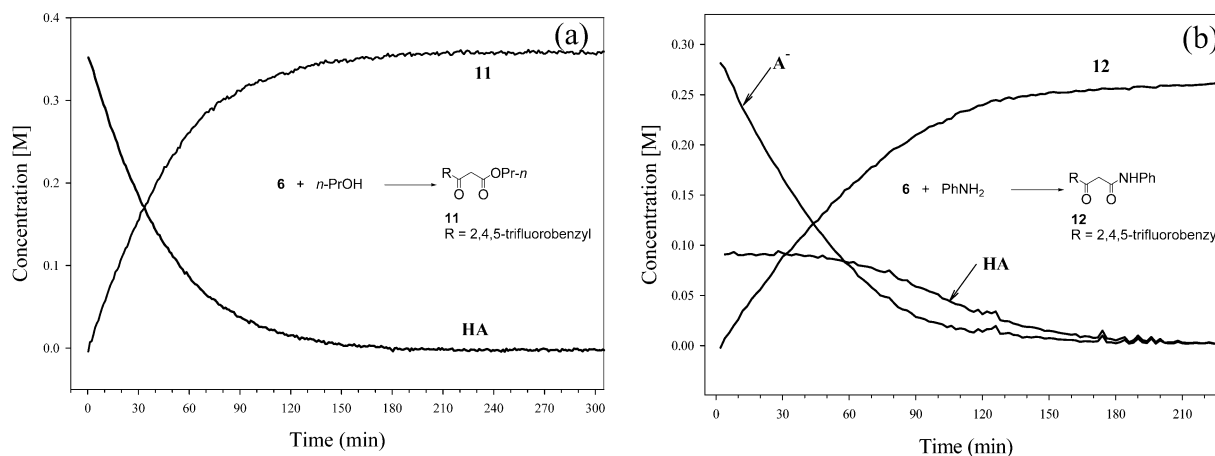
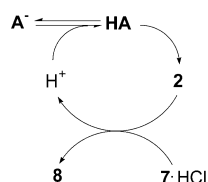


**Figure 5.** Plots of concentration of free acid and anion forms of **6** and products in  $\text{Me}_2\text{NAC}$  vs time. Reaction conditions: (a) *n*-PrOH at 51.0 °C; (b) aniline at 50.8 °C.

**Scheme 5.** Acid–Base–Salt Turning Cycle in the One-Pot Process



energies. In  $\text{Me}_2\text{NAC}$ ,  $\Delta G_{\text{obs}}^\ddagger = 23.9, 24.0, 24.1$  kcal/mol at 61.8, 51.4, and 41.1 °C, respectively.  $\Delta H_{\text{obs}}^\ddagger$  was 27.1 kcal/mol and  $\Delta S_{\text{obs}}^\ddagger$  was  $9.6 \pm 1$  eu. The observed positive  $\Delta S_{\text{obs}}^\ddagger$  in  $\text{Me}_2\text{NAC}$  clearly shows that a dissociative transition state is involved during the decarboxylation of acyl Meldrum's adducts. This is consistent with the hypothesis that the rate-determining step is formation of  $\alpha$ -oxoketene rather than an intermolecular nucleophilic addition–elimination mechanism.

**Kinetic Profile in the Process Solution.** Finally, the kinetic profiles in the process solution used for the synthetic reaction were examined. In these experiments, amine HCl salts were used. As mentioned above, 1 equiv of *t*-BuCO<sub>2</sub>H and 1 equiv of HCl are formed during the formation of **6**. The 2 equiv of *i*-Pr<sub>2</sub>NEt charged at the beginning of the reaction is thus used to neutralize the 1 equiv of HCl and 1 equiv of free acid **6** to their corresponding salts. Maintaining **6** as its anionic form is one of the keys to making this process robust by minimizing its decomposition, since **6** remains as its anionic form in the solution until a catalytic amount of TFA is added. TFA provides the proton source to partially convert the anionic form of **6** to its free acid while TFA in turn is converted to its carboxylate salt. As the decarboxylation of **6** proceeds, the triazole HCl salt **7** is converted to amide **8** while the liberated H<sup>+</sup> converts the anionic form of **6** to its free acid form. With this overall acid–base–salts turnover cycle (Scheme 5) in mind, the outcome of the kinetic results for the real process can be readily understood.

The requirement of 1 full equiv of TFA to complete the self-decomposition of **6** in the process solution confirms the acid–base turnover cycle. Addition of TFA converts the anionic form of **6** into its free acid which initiates decomposition. NMR analyses of the decomposed products indicated that polymers or oligomers were formed. The reaction profile by online IR clearly showed that **6** decomposed after aliquots of TFA were introduced sequentially (Figure 6). Kinetic analysis indicated

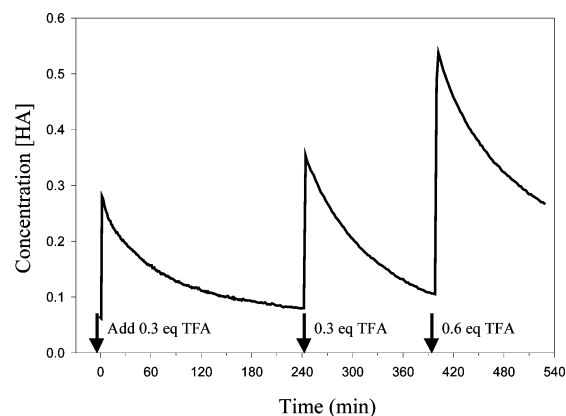


**Figure 6.** Plot of concentration of the acid form of **6** vs time for self-decomposition of **6** in MeCN process solution at 49.5 °C.

**Table 2.** Measured  $k_{\text{obs}}$ 's in MeCN Process Solution<sup>a</sup>

entry	substrates	$k_{\text{obs}} \times 10^{-4} (\text{s}^{-1})$	$T$ (°C)	yield <sup>c</sup> (%)
1	PhNH <sub>2</sub> <sup>b</sup>	2.93	48.5	12, 92
2	7 <sup>b</sup>	2.74	49.5	8, 91
3	7 <sup>b,d</sup>	3.30	49.6	8, 90
4	none <sup>e</sup>	2.13	49.5	
5	none <sup>e</sup>	2.16	49.5	
6	none <sup>e</sup>	1.48	49.5	

<sup>a</sup> Unless otherwise mentioned, a process stock solution of **6** was prepared from 1.0 equiv of Meldrum's acid, 2.15 equiv of *i*-Pr<sub>2</sub>NEt, 1.1 equiv of pivaloyl chloride, and 0.08 equiv of DMAP. 0.3 equiv of TFA was charged after HCl salt **7** or aniline HCl salt was added. <sup>b</sup> HCl salt. <sup>c</sup> Assay yield calculated by HPLC using an external reference standard. <sup>d</sup> 0.5 equiv of TFA was charged. <sup>e</sup> Self-decomposition of **6** in the process MeCN solution by stepwise addition of TFA: entry 4, with first 0.3 equiv of TFA addition; entry 5, with second 0.3 equiv of TFA addition; entry 6, with last 0.6 equiv of TFA addition.

first order in [HA] and zero in [A<sup>-</sup>] (Figure S7, Supporting Information). The  $k_{\text{obs}}$ 's measured at each of the three TFA charge stages are listed in Table 2 (entries 4–6).

Figure 7 shows the kinetic profile under the actual process conditions. The reaction profile (combination of the anion and free acid of **6** vs time) obtained by HPLC analysis also matched the online IR data. Again, use of online IR coupled with principal component analysis provided the means to profile HA and A<sup>-</sup> during the reaction. Formation of the free acid form **6** (HA) was immediately observed upon addition of a catalytic amount of TFA. This clearly shows that constant liberation of the free acid form HA through a fast acid–base proton exchange

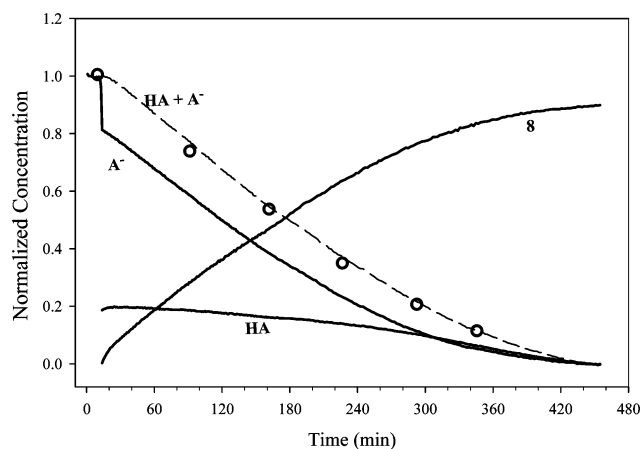


**Figure 7.** Plots of concentration of the free acid and anion forms of **6** and **8** in MeCN process solution vs time. Reaction conditions: 0.3 equiv of TFA and 1.0 equiv of triazole HCl salt **7** at 49.5 °C. [HA] plus [A<sup>-</sup>]: dashed line is based on online IR data. Circles are obtained by HPLC analyses. For the reaction sequence, see Scheme 5.

during the reaction is the key to achieve high conversion (>99%). This is also consistent with the observed variation in decarboxylation rate and conversion if TFA is not introduced into the reaction system since any excess base would prevent complete conversion to the free acid form.

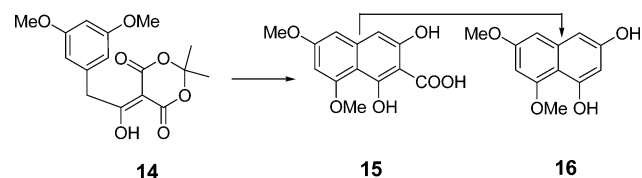
Under process conditions, the decarboxylation is pseudo zero order in the anionic form **6**, which is the same as when isolated **6** is treated with free amine nucleophiles in Me<sub>2</sub>NAc. The reaction rate increases as more TFA is charged, because the initial concentration of **HA** is increased. However, the  $k_{\text{obs}}$ 's are almost the same (Table 2, entries 2 and 3). Use of aniline HCl salt instead of triazole HCl salt **7** does not affect the reaction rate (Table 2, entry 1), which is consistent with previous observations. The data are consistent with the rate-determining step being the formation of the  $\alpha$ -oxoketene intermediate **2** under the one-pot conditions developed for synthetic applications.

**Attempts To Directly Observe  $\alpha$ -Oxoketene Species.** The decarboxylation step was also studied by using a special IR probe (Sicomp) in an attempt to detect ketene-related intermediates. However, in the presence or absence of triazole HCl salt **7** with various TFA charges, no ketene species could be detected by online IR. This is not surprising and is consistent with our kinetic results which showed the decarboxylation to form the  $\alpha$ -oxoketene step is the rate-determining step and there is no accumulation of  $\alpha$ -oxoketene intermediate in the reaction solution.<sup>32</sup>

**Model and Bridging Studies.** Thus far, the kinetic data outlined above are consistent with formation of an  $\alpha$ -oxoketene that arises from the free acid form, **HA**. Although the reaction is conducted under acidic conditions, the kinetics are consistent with reaction via the free acid **HA**, not the protonated acid **H<sub>2</sub>A<sup>+</sup>**. To determine if the protonated acyl Meldrum's adduct **H<sub>2</sub>A<sup>+</sup>** and the protonated ketene are viable intermediates under the conditions used in the process described above, a model study was designed to trap the intermediates. It has been reported

(32) Hydration, aminolysis, and alcoholysis of ketenes are fast reactions. In comparison of the reaction rate constants the self-decomposition of **6** with reported  $k$  for hydration, or aminolysis, or alcoholysis of ketenes, the reaction rate difference could be up to 10 orders of magnitude. (a) Chiang, Y.; Guo, H.-X.; Kresge, A. J.; Tee, O. S. *J. Am. Chem. Soc.* **1996**, *118*, 3386-3391. (b) Allen, A. D.; Andoas, J.; Kresge, A. J.; McAllister, M. A.; Tidwell, T. T. *J. Am. Chem. Soc.* **1992**, *114*, 1878-1879.

**Table 3.** Preparation of Diphenol **15** and **16**<sup>a</sup>

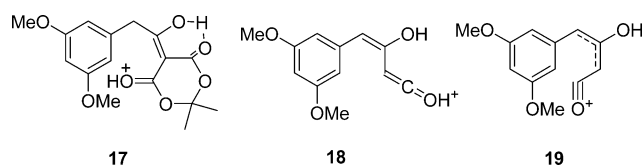


entry	conditions	ratio of <b>15/16</b>	yield (%)
1	<b>14</b> , TFA (1 equiv), 55 °C, 3 h	>98:2	<b>15</b> , <sup>b</sup> 70
2	<b>14</b> , TFA (0.5 equiv), Et <sub>3</sub> N·HCl (1 equiv), 55 °C, 3 h	7.4:1	<b>15</b> + <b>16</b> , <sup>b</sup> 70
3	<b>14</b> , 55 °C, 1 h 4.5 h 24 h	8:1 0.9:1 0:100	<b>16</b> , <sup>b</sup> 72
4	<b>15</b> , TFA (0.5 equiv), Et <sub>3</sub> N·HCl (1 equiv), 55 °C, 24 h	4:1	
5	<b>15</b> , TFA (0.5 equiv), 24 h	98:2	

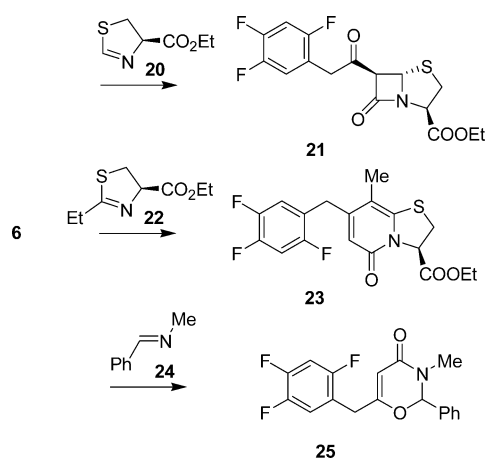
<sup>a</sup> The main purpose of adding TFA or triethylamine HCl salt is to mimic the one-pot process conditions. <sup>b</sup> Isolated yield. <sup>c</sup> Assay yield calculated by HPLC using an external reference standard.

that malonate derivatives can be used as acylating reagents with aromatic compounds via Friedel–Crafts-type reactions under acidic conditions.<sup>33</sup> Most likely, this type of reaction occurs through a protonated intermediate. To probe the existence of protonated acyl Meldrum's adducts, compound **14** was prepared and subjected to decarboxylation in the absence of an external nucleophile.

As shown in Table 3, entries 3 and 4, only minor amounts of **16** are formed initially, and it grows in as the reaction proceeds at the expense of **15**. Clearly, **16** is formed by decarboxylation of **15** under the reaction conditions, although decarboxylation by enolation can be suppressed in the presence of a strong acid (Table 3, entries 1 and 5). Therefore, formation of **16** does not provide evidence for a reaction pathway through a protonated ketene (such as **18** or **19**) or ketene intermediate; in contrast, the fact that the ratio of **16/15** is suppressed to 2:98 in the presence of TFA indicates that formation of **16** is from direct cyclization of the protonated **17**. When reaction of **14** is carried out in the absence of additional acid (entry 3), **17** could only arise via protonation by acyl Meldrum's acid **14** itself, followed by Friedel–Crafts-type reaction with the electron-rich aromatic ring.<sup>14</sup> It is also possible that unprotonated **14** is sufficiently reactive such that protonation is not required for cyclization to occur. To summarize, this intramolecular trapping experiment indicated that protonated intermediate **17** (**H<sub>2</sub>A<sup>+</sup>**) is a possible intermediate in these reactions, but provided no evidence for the formation of protonated ketene intermediates such as **18** and **19**.



**Bridging Studies with Other Substrates.** Up to now we have described reactions of Meldrum's adducts with various nucleophiles including amines of varying basicity and nucleophilicity, alcohols, and carbamates. Reactions with imines have been reported in the literature, but under conditions quite

**Scheme 6.** Reaction of **6** with Imines

different from those we developed for the keto-amide formation. We wanted to determine if the experimental conditions we were operating under for keto-amide and keto-ester formation could be bridged to those reported in the literature for reaction with imines, since different pathways may be involved for the same substrate under different reaction conditions. We chose the imines **20**, **22**, and **24** since they have been reported in previous studies (Scheme 6).

A mixture of 2 equiv of **6** and 1 equiv of thiazoline **20** was saturated with HCl(g) and aged in refluxing benzene as described in the literature for preparation of  $\beta$ -lactams.<sup>3</sup> The desired  $\beta$ -lactam **21** was isolated in 41% yield.<sup>29</sup> Similarly, treatment of **6** with the substituted  $\Delta^2$ -thiazoline **22** in HCl(g)-saturated 1,2-dichloroethane at 65 °C for 3 h gave the pyridinone **23** in 80% yield.<sup>29</sup> The above two reactions were also carried out in the absence of HCl(g). Although the reaction did not proceed as cleanly as in the presence of HCl(g), formation of the  $\beta$ -lactam **21** and pyridinone **23** was clearly observed, respectively. These control experiments confirmed that HCl(g) is not necessary to lead to formation of the  $\beta$ -lactam or pyridinone in both cases.

When **6** was treated with *N*-benzylidene methylamine (**24**) in MeCN at 55 °C for 5 h instead of in refluxing benzene,<sup>6a</sup> the expected product **25** was also obtained.<sup>34</sup> Since the same products are generated under either our conditions or those

reported in the literature, we conclude that for the same substrate, decarboxylation of acyl Meldrum's adducts is likely occurring through the same reaction pathway.

## Conclusion

A practical one-pot process for preparation of  $\beta$ -keto amides has been developed. Use of online IR and subsequent principal component analysis for kinetic studies were critical as a tool for profiling the concentration changes of the anion and free acid forms, as well as the product, throughout the course of the reaction. Kinetic mechanistic studies clearly revealed that formation of  $\beta$ -keto amides from acyl Meldrum's adducts were generated via the  $\alpha$ -oxoketene intermediate **2** either under synthetically relevant reaction conditions or in a "clean" system, in which only isolated acyl Meldrum's adduct **6** and amine free base were involved. The formation of  $\alpha$ -oxoketene was also demonstrated by kinetic studies on the self-decomposition of acyl Meldrum's adducts under a variety of conditions. The anionic form  $A^-$  was shown to be stable and not directly involved in nucleophilic addition or self-decomposition, while the free acid form **HA** was responsible for generating  $\alpha$ -oxoketene intermediate **2**. The possibility of protonated  $\alpha$ -oxoketene intermediates involvement in the formation of  $\beta$ -keto amides was unambiguously ruled out based on the observed kinetic profiles. Our kinetic studies on acyl Meldrum's acid **6** with various substrates (such as carbamates, alcohols, and amines) and the "bridging" studies on the thiazolines also clearly demonstrated that  $\alpha$ -oxoketene intermediates are the main reaction pathway. However, if a nucleophile or a substrate is able to react with  $H_2A^+$  before it can be converted to an  $\alpha$ -oxoketene intermediate, then the pathway to trap the protonated acyl Meldrum's acids becomes possible and formation of products such as **15** and 1,3-oxazinones<sup>6</sup> could be observed.

**Supporting Information Available:** All kinetic profiles, experimental procedures, and spectral data of **6** and **8**. This material is available free of charge via the Internet at <http://pubs.acs.org>.

JA046488B

(33) (a) Piettre A.; Chevenier, E.; Masardier, C.; Gimbert, Y.; Greene, A. *Org. Lett.* **2002**, *4*, 3139–3142. (b) Plazuk, D.; Zakrzewski, J. *J. Org. Chem.* **2002**, *67*, 8672–8674.

(34) See ref 6a. Yamamoto et al. confirmed oxazin-4-ones are formed if acyl Meldrum's acids are subjected to the same reaction conditions.